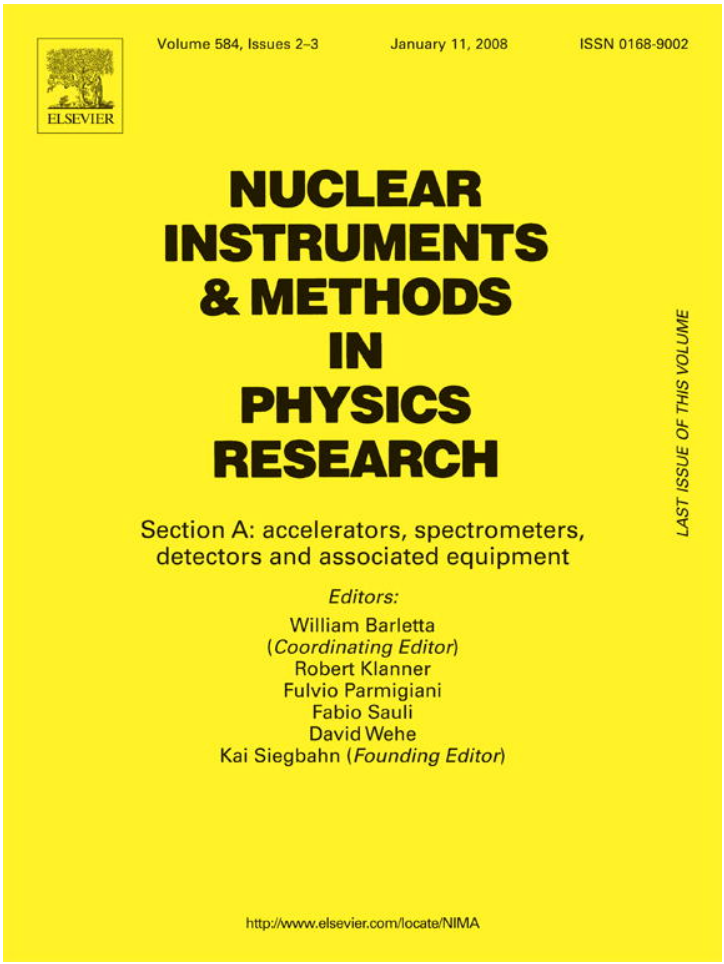

Available online at www.sciencedirect.com
ScienceDirect
Nuclear Instruments and Methods in Physics Research A 584 (2008) 334–345
NUCLEAR INSTRUMENTS & METHODS IN PHYSICS RESEARCH Section A
www.elsevier.com/locate/nima

Development of $CaMoO_4$ crystal scintillators for a double beta decay experiment with ^{100}Mo

A.N. Annenkov[a], O.A. Buzanov[a], F.A. Danevich[b,*], A.Sh. Georgadze[b], S.K. Kim[c], H.J. Kim[d], Y.D. Kim[e], V.V. Kobychev[b], V.N. Kornoukhov[f], M. Korzhik[g], J.I. Lee[e], O. Missevitch[g], V.M. Mokina[b], S.S. Nagorny[b], A.S. Nikolaiko[b], D.V. Poda[b], R.B. Podviyanuk[b], D.J. Sedlak[b], O.G. Shkulkova[b], J.H. So[d], I.M. Solsky[h], V.I. Tretyak[b], S.S. Yurchenko[b]

[a]*Moscow Steel and Alloy Institute, 119049 Moscow, Russia*
[b]*Institute for Nuclear Research, MSP 03680 Kyiv, Ukraine*
[c]*DMRC and School of Physics, Seoul National University, Seoul 151-742, Republic of Korea*
[d]*Physics Department, Kyungpook National University, Daegu 702-701, Republic of Korea*
[e]*Sejong University, Seoul, Republic of Korea*
[f]*Institute for Theoretical and Experimental Physics, 117218 Moscow, Russia*
[g]*Institute for Nuclear Problems, 220030 Minsk, Belarus*
[h]*Institute for Materials, 79031 Lviv, Ukraine*

Received 11 July 2007; received in revised form 11 September 2007; accepted 25 October 2007
Available online 5 November 2007

Abstract

We have studied the energy resolution, α/β ratio, temperature dependence of the scintillation properties, and the radioactive contamination of $CaMoO_4$ crystal scintillators. We have also examined the use of pulse-shape discrimination to distinguish γ rays and α particles. A high sensitivity experiment to search for the $0\nu2\beta$ decay of ^{100}Mo using $CaMoO_4$ scintillators is discussed.

PACS: 23.40.−s; 29.40.Mc

Keywords: Double beta decay; Scintillation detector; $CaMoO_4$ crystals; Pulse-shape discrimination; Radiopurity

1. Introduction

It has been already demonstrated by several experiments that scintillation detectors are a promising tool to search for the double beta (2β) decay processes; some examples of their application can be found in Refs. [1–10]. Scintillation detectors possess a range of important characteristics for a high sensitivity 2β decay experiment: high registration efficiency for 2β processes, reasonable energy resolution, the potential to use pulse-shape discrimination to reduce the background, operating stability, and low cost. There exists a few detector materials containing molybdenum. The most promising of them, from the point of view of light output, is calcium molybdate ($CaMoO_4$). In Ref. [11] $CaMoO_4$ crystal scintillators were proposed to search for the neutrinoless (0ν) 2β decay of ^{100}Mo. Recently $CaMoO_4$ has been intensively studied for possible use in a cryogenic scintillation-bolometric detector for experiments to search for 2β decay and dark matter [12–17].

^{100}Mo is one of the most promising candidates for 2β decay experiments because of its high transition energy ($Q_{2\beta} = 3035$ keV). As a result, the calculated value of the phase space integral $G^{0\nu}_{mm}$ of the $0\nu2\beta$ decay of ^{100}Mo is one

*Corresponding author. Tel.: +380 44 525 1111; fax: +380 44 525 4463.
E-mail address: danevich@kinr.kiev.ua (F.A. Danevich).

0168-9002/$ - see front matter © 2007 Elsevier B.V. All rights reserved.
doi:10.1016/j.nima.2007.10.038

of the largest among 35 possible $2\beta^-$ decay candidates [18,19]. Theoretical predictions for the product of the half-life and the squared effective neutrino mass $T^{0\nu}_{1/2} \cdot \langle m_\nu \rangle^2$ are in the range of 8.0×10^{22}–4.1×10^{24} yr eV^2 (see compilations [20] and more recent calculations [21]).[1] Further, from an experimental point of view, the larger is the $Q_{2\beta}$ energy, the simpler it is to overcome background problems, in particular, because the background from natural radioactivity drops sharply above 2615 keV, the energy of γ's from ^{208}TI decay (^{232}Th family). In addition, cosmogenic activation, which is important for the next generation of 2β decay experiments (see, for instance [23]), contributes less at higher energies.

Two neutrino double beta decay ($2\nu2\beta$) of ^{100}Mo to the ground state of ^{100}Ru has already been observed in several direct detection experiments [24,25] with measured half-lives in the range of $3.3 \times 10^{18} - 1.2 \times 10^{19}$ yr; the most recent value from the NEMO-3 experiment is based on 219,000 detected $2\nu2\beta$ events and is equal to $T_{1/2} = 7.1 \pm 0.5 \times 10^{18}$ yr [25]. Geochemical measurements gave the value of $T_{1/2} = 2.2 \pm 0.3 \times 10^{18}$ yr [26]. In addition to transition to the ground state, the $2\nu2\beta$ decay of ^{100}Mo to the first excited 0^+_1 level of ^{100}Ru ($E_{\rm exc} = 1131$ keV) has also been observed; measured values of half-lives are in the range of $(5.7-9.3) \times 10^{20}$ yr [27]. New studies of this mode are also in progress [28]. The neutrinoless 2β decay has yet not been observed: the best limit, reached in the NEMO-3 experiment, is $T_{1/2} > 4.6 \times 10^{23}$ yr at 90% C.L. [25].

The purpose of our work was investigation of the energy resolution, light yield, α/β ratio, pulse shapes (for γ rays and α particles), temperature dependence of the scintillation properties, and the pulse-shape discrimination ability of a few samples of $CaMoO_4$ crystal scintillators produced by the Institute for Materials (IM, Lviv, Ukraine), and by the Innovation Centre of the Moscow Steel and Alloy Institute (ICMSAI, Moscow, Russia). Radioactive contamination of four samples of $CaMoO_4$ crystals was tested in the Solotvina Underground Laboratory.

2. Samples

The main properties of $CaMoO_4$ scintillators are presented in Table 1, where the characteristics of calcium and cadmium tungstates are also given for comparison. The material is non-hygroscopic and chemically resistant. Five clear, practically colourless $CaMoO_4$ crystals were used in our studies. The scintillators were fabricated from single crystals grown by the Czochralski method. All crystals used in the present study are listed in Table 2. The samples CMO-2, CMO-3, and CMO-4 have not exactly cylindrical shape. For this reason the mass of the crystals are slightly different.

[1] One very different result is also known: 3.6×10^{27} yr eV^2 in accordance with Ref. [22].

Table 1
Properties of $CaMoO_4$, $CaWO_4$, and $CdWO_4$ crystal scintillators

	$CaMoO_4$	$CaWO_4$ [29]	$CdWO_4$ [30]
Density (g/cm^3)	4.2–4.3 [31]	6.1	8.0
Melting point (°C)	1445–1480 [32]	1570–1650	1325
Structural type	Scheelite [33]	Scheelite	Wolframite
Cleavage plane	Weak (0 0 1) [33]	Weak (1 0 1)	Marked (0 1 0)
Hardness (Mohs)	3.5–4 [31]	4.5–5	4–4.5
Wavelength of emission maximum (nm)	520 [11]	420–440	480
Refractive index	1.98 [31]	1.94	2.2–2.3
Effective average decay time[a] (μs)	14	8	13
Photoelectron yield [% of NaI(Tl)][a]	9%	18%	20%

[a] For γ rays, at room temperature.

3. Measurements and results

3.1. Energy resolution and relative light output

In the present work, the energy resolution was measured for all the $CaMoO_4$ samples.

The $CaMoO_4$ crystal (CMO-4) was roughened on the side surface using fine grinding paper, the exit and top surfaces were polished. The scintillator was wrapped with PTFE reflector tape and optically coupled to a 3 in. Philips XP2412 photomultiplier (PMT). The measurements were carried out with a home-made spectroscopy amplifier with 16 μs shaping time to collect most of the charge from the anode of the PMT. The scintillator was irradiated by γ quanta from ^{137}Cs, ^{207}Bi, ^{232}Th, and ^{241}Am sources. Energy resolutions (full width at half maximum, FWHM) of 34% (^{241}Am, 60 keV), 10.3% (^{137}Cs, 662 keV), 7.7% (^{207}Bi, 1064 keV), and 4.7% (^{208}TI, 2615 keV) were measured (see Fig. 1). The energy resolution obtained in the present study is the best ever reported for $CaMoO_4$ crystal scintillators. It is important to stress that the clear peak of the 2615 keV γ line of ^{208}TI (^{232}Th source) was measured. It demonstrates a possibility to calibrate the energy scale of a $CaMoO_4$ detector in the vicinity of the expected peak of $0\nu2\beta$ decay of ^{100}Mo using a ^{228}Th source.

The dependence of the energy resolution and light output on the surface treatment was checked with the sample CMO-5. First, all surfaces of the crystal were polished. An energy resolution of 16.2% was measured in these conditions for the ^{137}Cs 662 keV γ line. Then the surface of the crystal, except the exit window connected to the PMT, was roughened with fine-grained grinding paper. The relative pulse amplitude increased by 1.21 times and the energy resolution improved to 14.0%.

The relative light output of the $CaMoO_4$ crystal (CMO-4) was measured relatively to the $CaWO_4$ scintillator

Table 2
Samples of $CaMoO_4$ crystal scintillators used in this study and their scintillation properties

ID	Size (mm)	Mass (g)	Manufacturer	Relative pulse amplitude (%)	FWHM at 662 keV (%)
CMO-1	$25 \times 13 \times 9$	11.5	IM[a]	100	12.8[b]
CMO-2	$\oslash 38 \times 20$	95.6	IM[a]	103	12.5[c]
CMO-3	$\oslash 38 \times 20$	99.9	IM[a]	110	11.9[c]
CMO-4	$\oslash 38 \times 20$	97.8	IM[a]	118	10.3[c]
CMO-5	$28 \times 28 \times 24$	82.5	ICMSAI[d]	79	14.0[b]

[a]Institute for Materials (Lviv, Ukraine).
[b]Exit surface (coupled to PMT) was polished; other surfaces were diffused.
[c]Exit and opposite surfaces were polished; side surface was diffused.
[d]Innovation Centre of the Moscow Steel and Alloy Institute (Moscow, Russia).

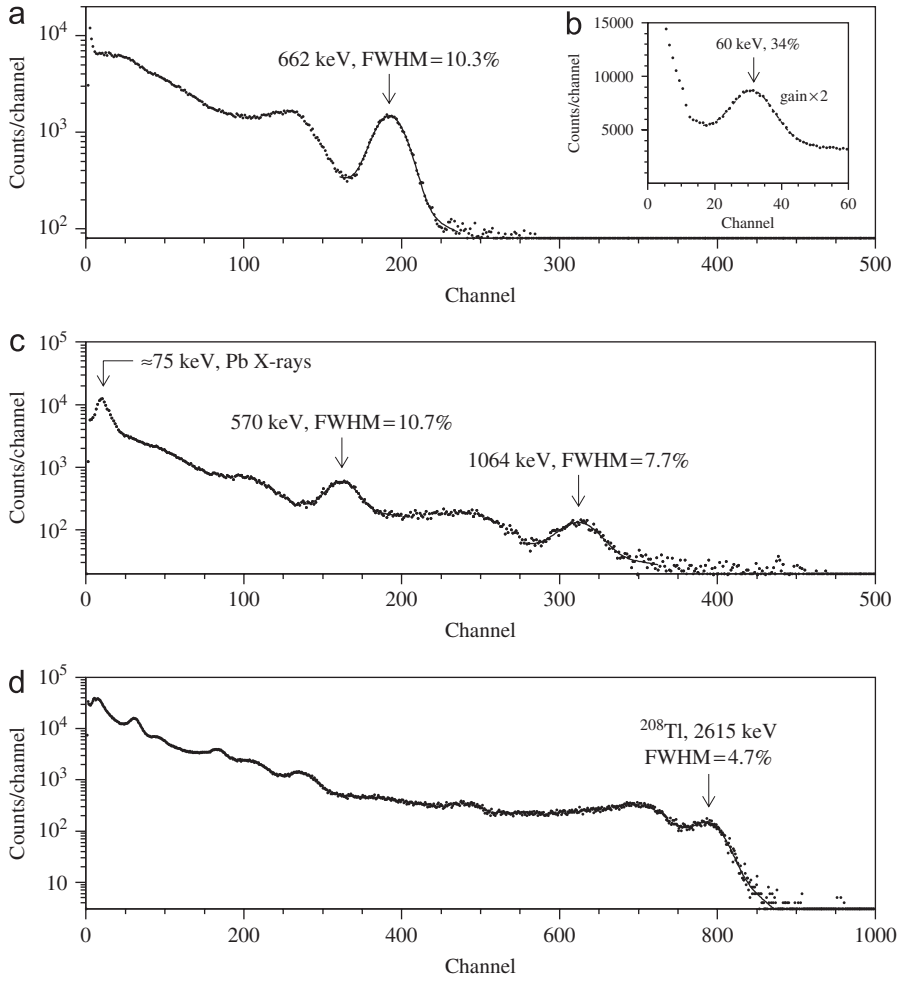

Fig. 1. Energy spectra of ^{137}Cs (a), ^{241}Am (b), ^{207}Bi (c), and ^{232}Th (d) γ quanta measured with $CaMoO_4$ scintillation crystal $\oslash 38 \times 20$ mm (CMO-4).

$\oslash 40 \times 39$ mm [29] with the help of the same experimental technique as 36%.

The light output of the CMO-4 scintillator was also measured relatively to a NaI(Tl) scintillator $\oslash 40 \times 40$ mm of standard assembly. To account for the substantial difference in the scintillation decay times of $CaMoO_4$ (14 μs) and NaI(Tl) (0.25 μs), the energy spectra were built by calculating the areas of pulses (over 300 μs for $CaMoO_4$ and 6 μs for NaI(Tl)) accumulated using a 20 MS/s transient digitizer based on the 12 bit ADC (AD9022) [34]. The photoelectron yield of 8% relatively to NaI(Tl) was obtained for the CMO-4 sample.

3.2. α/β ratio

The α/β ratio was measured with the CMO-1 crystal using collimated α particles of a ^{241}Am source. The dimensions of the collimator were $\oslash 0.75 \times 2$ mm. As it

was checked by a surface-barrier detector, the energy of α particles was reduced to about 5.25 MeV by 2 mm of air due to passing through the collimator [35]. Fig. 2 shows the energy spectrum of the α particles measured by the $CaMoO_4$ scintillator. The α/β ratio is 0.20 at the energy of α particles 5.25 MeV.

Besides the measurements with the external source, α peaks of ^{220}Rn and ^{216}Po (from the ^{232}Th chain), and ^{210}Po and ^{214}Po (^{238}U), present in trace amounts in the $CaMoO_4$ crystal (⌀38 × 20 mm, CMO-2), were used to extend the energy range of α particles. The peaks of ^{220}Rn, ^{216}Po, and ^{214}Po were selected with the help of the time–amplitude analysis of data obtained in the low background measurements (see Section 3.6.3). The peak of ^{210}Po is clearly present in the energy spectrum of the $CaMoO_4$ detector (Section 3.6.2). The measured dependence of the α/β ratio on the energy of α particles (Fig. 3) can be described in the energy region 5−8 MeV by the linear function: $\alpha/\beta = 0.11(2) + 0.019(3)E_\alpha$, where E_α is energy of α particles in MeV. The α/β ratio measured with external α source is lower than those obtained with internal α's. It can be explained by some difference in light collection from the ^{241}Am source (placed on the top of the crystal) in comparison with uniformly distributed scintillations from internal α decays, effect of surface treatment, etc.

As the quenching of the scintillation light caused by α particles (in comparison with electrons) is due to the higher ionization density of α particles, such a behaviour of the α/β ratio can be explained by the energy dependence of ionization density of α particles [36].

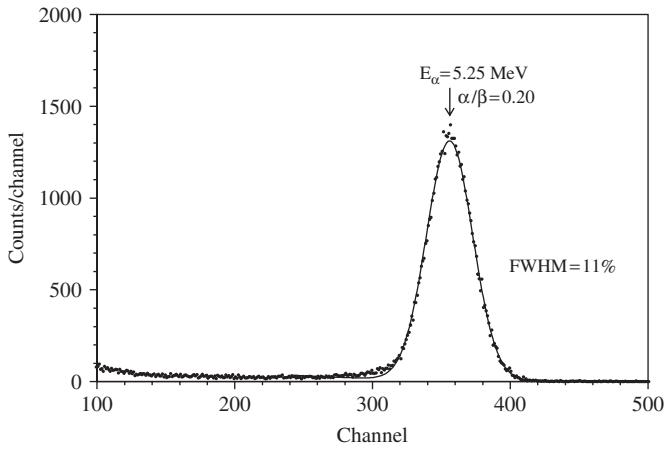

Fig. 2. The energy spectrum measured with 5.25 MeV α particles from an ^{241}Am source (dots). Fit of the α peak is shown by solid line.

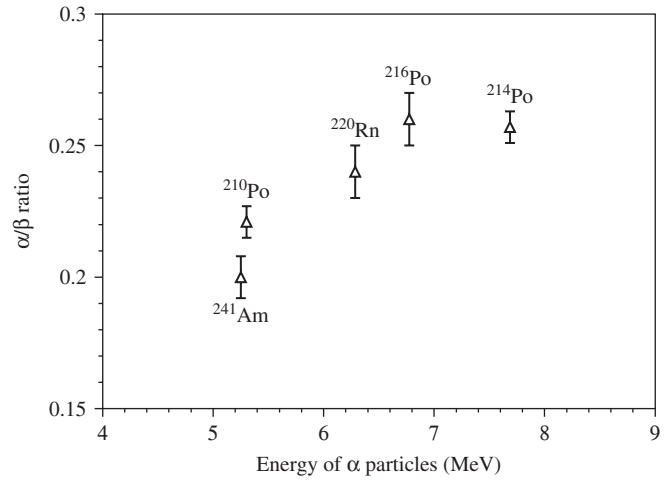

Fig. 3. Dependence of the α/β ratio for $CaMoO_4$ on the energy of α particles.

3.3. Pulse shape for γ rays and α particles

The pulse shapes measured using the $CaMoO_4$ scintillator (CMO-1) were studied using the 12 bit 20 MS/s transient digitizer. To study the pulse shape of scintillation decay for α particles, the $CaMoO_4$ crystal was irradiated by α particles from collimated ^{241}Am source. A ^{60}Co source was used to investigate pulse shape for γ quanta. These measurements were carried out at the temperature (27 ± 1) °C.

The shape of the light pulses produced by α particles and γ rays in the $CaMoO_4$ scintillator are shown in Fig. 4. To obtain the pulse shapes, about 1000 of individual α(γ) events with amplitudes corresponding to the α peak of ^{241}Am were summed. The pulses were fitted by the function:

$$f(t) = \sum A_i(e^{-t/\tau_i} - e^{-t/\tau_0})/(\tau_i - \tau_0), \quad t > 0$$

where A_i are the relative intensities, τ_i are the decay constants for different light-emission components, and τ_0 is integration constant of the electronics ($\tau_0 \approx 0.08$ μs). Three decay components were observed with $\tau_i \approx 0.3-1$, ≈ 4, and ≈ 17 μs with different intensities for γ rays and α particles (see Fig. 4 and Table 3).

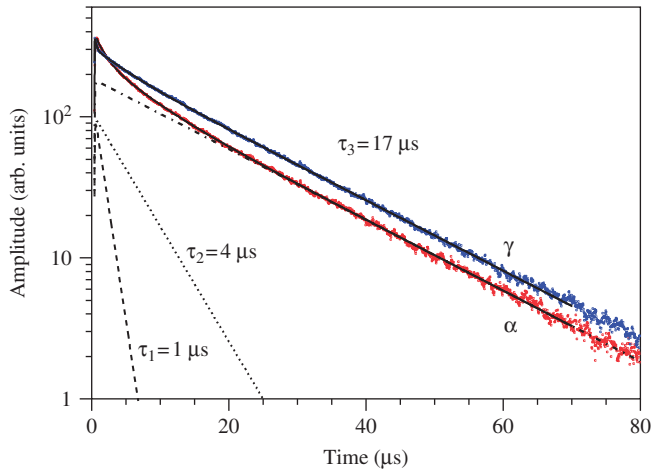

Fig. 4. Decay of scintillation in a $CaMoO_4$ crystal for γ rays and α particles. Three components of scintillation signals for α particles with decay constants of 1, 4, and 17 μs are shown. Fitting functions for α and γ pulses are drawn by solid lines.

Table 3
Decay time of $CaMoO_4$ scintillators for γ quanta and α particles at +27 °C

Type of irradiation	Decay constants and relative intensities		
	$\tau_1(A_1)$	$\tau_2(A_2)$	$\tau_3(A_3)$
α particles	1 μs (2%)	4 μs (13%)	17 μs (85%)
γ rays	0.3 μs (0.5%)	4 μs (5.5%)	17 μs (94%)

The decay constants and their relative intensities are denoted as τ_i and A_i, respectively.

3.4. Pulse-shape discrimination between γ rays and α particles

The difference between the pulse shapes allows us to discriminate γ(β) events from those induced by α particles. We applied for this purpose the optimal filter method proposed in Ref. [37], and successfully used for different scintillation detectors: $CdWO_4$ [30,34], CeF_3 [7], $CaWO_4$ [29], YAG:Nd [38], $ZnWO_4$ [9], CaF_2(Eu) [39], and $PbWO_4$ [40]. For each $CaMoO_4$ signal, a numerical characteristic (shape indicator, SI) was calculated in the following way:

$$\mathrm{SI} = \sum f(t_k)P(t_k) \Big/ \sum f(t_k)$$

where the sum is over time channels k, from the origin of pulse and up to 50 μs, $f(t_k)$ is the digitized amplitude (at the time t_k) of the signal. The weight function $P(t)$ was defined as: $P(t) = \{f_\alpha(t) - f_\gamma(t)\}/\{f_\alpha(t) + f_\gamma(t)\}$, where $f_\alpha(t)$ and $f_\gamma(t)$ are the reference pulse shapes for α particles and γ quanta.

Reasonable discrimination between α particles and γ rays was achieved using this approach, as one can see in Fig. 5 where the scatter plot of the shape indicator versus energy measured with the $CaMoO_4$ crystal CMO–1 for α particles ($E_\alpha \approx 5.25$ MeV) and γ quanta (≈ 1 MeV) are shown. As a measure of discrimination ability (factor of merit, FOM), the following expression can be used:

$$\mathrm{FOM} = |\mathrm{SI}_\alpha - \mathrm{SI}_\gamma| \Big/ \sqrt{\sigma_\alpha^2 + \sigma_\gamma^2},$$

where SI_α and SI_γ are mean SI values for α particles and γ quanta distributions (which are well described by Gaussian functions), σ_α and σ_γ are the corresponding standard deviations. For the distributions presented in inset of Fig. 5, the factor of merit FOM = 2.2.

3.5. Temperature dependence of light output and pulse shape

The temperature dependence of the scintillation properties was studied in the range $-158 \div +25$ °C with the CMO-1 sample. The crystal was viewed by the XP2412 PMT through a high purity quartz light-guide 4.9 cm in diameter and 25 cm long. The $CaMoO_4$ scintillator and the light-guide were wrapped with PTFE tape as a reflector. Dow Corning Q2-3067 optical couplant was used to provide optical contact of the scintillator with the light-guide, and of the light-guide with the PMT. The crystal and the main part of the light-guide were placed into a Dewar vessel, while the PMT was isolated from the vessel with the help of a foam plastic plate. This way the temperature of the PMT was kept stable (practically at room temperature) during the measurements. The Dewar vessel was periodically filled by small portions of liquid nitrogen to cool the detector. The temperature of the crystal was measured with a chromel–alumel thermocouple.

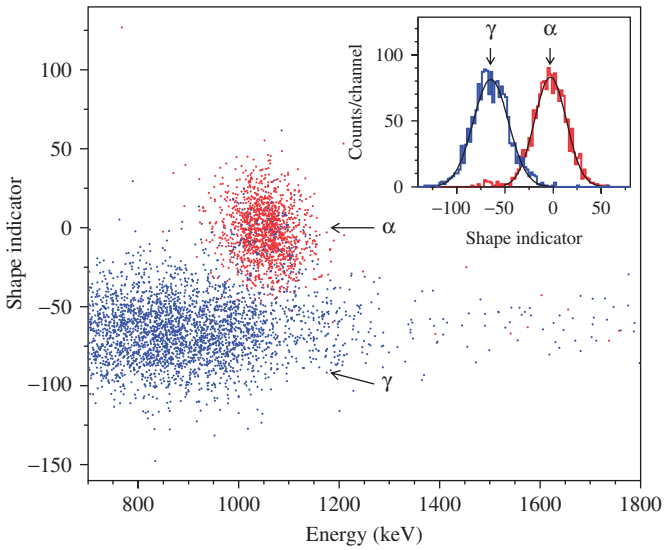

Fig. 5. Scatter plot of the shape indicator (see text) versus energy for a $CaMoO_4$ scintillation detector when irradiated by α particles (^{241}Am) and γ quanta (^{60}Co). (Inset) The shape indicator distributions measured for α particles and γ quanta. The distributions were fitted by Gaussian functions (solid lines).

To measure the relative light output and pulse shape, the scintillator was irradiated by α particles from the collimated ^{241}Am source ($E_\alpha = 5.25$ MeV). The 20 MS/s transient digitizer was used to accumulate 4000 scintillation pulse shapes of $CaMoO_4$ at each temperature. Then the recorded pulse shapes were used to build energy spectra and to determine the decay time. The energy spectra were obtained by calculating the area of each signal from the starting point up to 380 μs.

To present the dependence of scintillation decay of $CaMoO_4$ on temperature, we use the averaged decay time $\langle\tau\rangle$ determined by the following formula:

$$\langle\tau\rangle = \sum(\tau_i A_i) \Big/ \sum A_i.$$

The obtained dependence of the averaged decay time on temperature is presented in Fig. 6(a), and can be fitted in the temperature interval $-127 \div +25$ °C by the function $\langle\tau\rangle = 31.8(7) - 0.85(3) \times T + 0.0093(7) \times T^2$, where T is temperature in °C. At the temperature −50 °C (where the maximum of the light output was observed) the averaged decay time is ≈ 98 μs. The dependence of the averaged decay time on temperature of the $CaMoO_4$ scintillator agrees qualitatively with the result reported in Ref. [11]. Temperature dependence of the decay time constants is

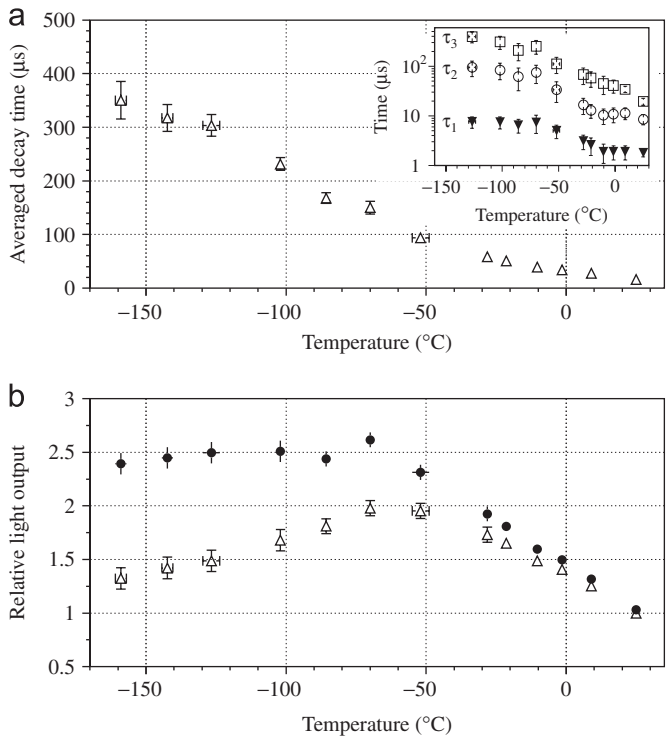

Fig. 6. (a) Temperature dependence of averaged decay time measured with a $CaMoO_4$ detector under irradiation by α particles from ^{241}Am source. (Inset) Temperature dependence of the decay time constants. (b) The dependence of relative light output on temperature (triangles). The data corrected to account for the decay time of the scintillation signals are shown by filled circles (see text).

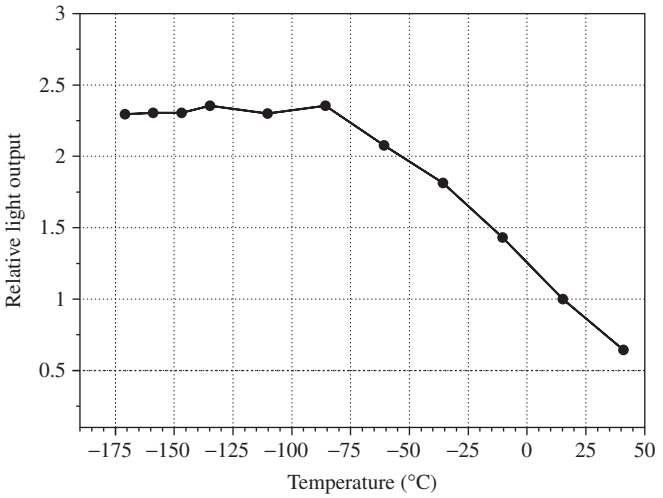

Fig. 7. Temperature dependence of radioluminescence intensity of $CaMoO_4$ crystal measured using the photon counting method.

presented in inset of Fig. 6. All three decay components increase with decrease of the temperature. Such a behaviour is in agreement with the results recently obtained in Ref. [41].

The measured dependence of the relative light output of the $CaMoO_4$ crystal scintillator on the temperature is presented in Fig. 6(b). The relative light output (RLO) increases as the temperature decreases down to $\approx -50\,^{\circ}C$ as $RLO = 1.374(16) - 0.0137(8) \times T - 0.00005(3) \times T^2$, where T is temperature in °C. Then some decrease of the scintillation intensity was observed. The dependence is in agreement with the result obtained in Ref. [11].

The temperature dependence of the radioluminescence intensity was also studied using the photon counting method. The dependence was measured in the temperature range $-170 \div +40\,^{\circ}C$ under γ-excitation by a ^{57}Co source. Light from the sample was directed to the PMT (FEU-100) input window through a condenser. The ^{57}Co source was installed at 8 cm distance from the sample. The PMT counting rate was averaged during 10 s at each value of the temperature. The dependence of the luminescence yield is presented in Fig. 7. It was found that as the temperature decreases down to $-80\,^{\circ}C$, the light yield increases by a factor of 2.5. The light yield remains practically unchanged as the temperature decreases further to $-170\,^{\circ}C$.

The difference in the temperature dependence of the light yield measured by two methods can be explained by the considerable increase of the scintillation decay time at temperatures lower than $\sim -50\,^{\circ}C$. Whereas the result of the photon counting method does not depend on the decay time, the relative light output measured using the transient digitizer depends on the kinetics of scintillation decay. To correctly calculate area of scintillation signals, the digitized pulses after 380 μs were reconstructed with the exponential function $f(t) = ae^{-t/\tau_i}$, with $\tau_i = \tau_3$, and amplitude a being a free parameter of the fit. After this effect was taken into account, the behaviour of the relative pulse amplitude measured with the help of the digitizer (the corrected data are presented in Fig. 6(b) by filled circles) are practically the same as measured with the photon counting method. The obtained data are in accordance with behaviour measured in Refs. [41,42].

3.6. Radioactive contamination

3.6.1. Set-up and measurements

The radiopurity of four samples (CMO-2, CMO-3, CMO-4, and CMO-5) was tested in the Solotvina Underground Laboratory built in a salt mine 430 m underground ($\simeq$ 1000 m of water equivalent) [43].

The crystals CMO-2, CMO-3, and CMO-4 were produced from a single boule with the aim of studying a possible dependence of radioactive contamination on the length of the boule. Such a dependence was observed for $CdWO_4$ crystals produced for the Solotvina experiment to search for 2β decay of ^{116}Cd [44]. The crystal CMO-2 was cut from the top of the boule (beginning of growth), the CMO-3 was taken from the middle part, and the CMO-4 sample was produced from the bottom part of the monocrystal boule.

The radioactive contamination of the $CaMoO_4$ crystals was measured in the low background set-up installed in the Solotvina Underground Laboratory. In the set-up a scintillation $CaMoO_4$ crystal was viewed by the

special low-radioactive 5 in. photomultiplier tube (EMI D724KFLB) through the high purity quartz light-guide $\oslash 10 \times 33$ cm. The detector was surrounded by a passive shield made of Teflon (thickness of 3–5 cm), Plexiglas (6–13 cm), high purity oxygen-free high conductivity copper (3–6 cm), lead (15 cm) and polyethylene (8 cm). For each event occurring in the detector, the amplitude of a signal and arrival time were recorded. In addition, $CaMoO_4$ scintillation pulse shapes were digitized with a 20 MHz sampling frequency in $\approx 100\,\mu$s full range. The energy scale of the detectors was calibrated using a ^{207}Bi γ source through the calibration channel made in the shield. The typical energy resolution of the CMO-2 crystal was FWHM 17.8% and 13.5% for 570 and 1064 keV γ lines, respectively.

3.6.2. Interpretation of background spectrum

The energy spectrum of the CMO-2 detector measured over a 74.83 h period in the low background set-up is presented in Fig. 8. The peak at energy ≈ 1.17 MeV can be attributed to intrinsic ^{210}Po (daughter of ^{210}Pb from the ^{238}U family) with activity of 0.42(1) Bq/kg. Apparently, the equilibrium of the uranium chain in the crystal was broken during crystal production, because in the spectrum there is no peak of ^{238}U expected at the energy of ≈ 0.82 MeV.

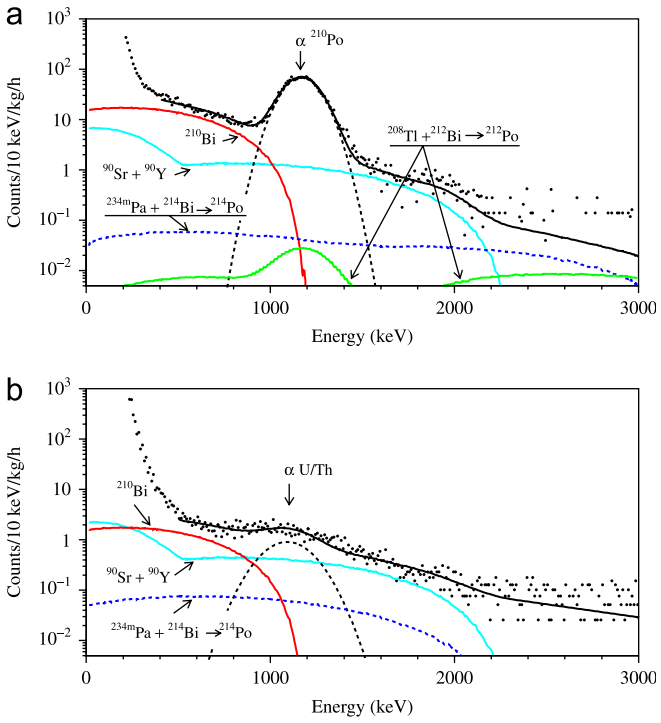

Fig. 8. (a) Energy spectrum of the $CaMoO_4$ scintillation crystal (CMO-2) measured in the low background set-up over 74.83 h. The peak with the energy ≈ 1.17 MeV is due to the α decay of ^{210}Po. (b) The spectrum measured over 472.4 h with the crystal CMO-5 in the same set-up. Both spectra are normalized on mass of the crystals and time of measurements. The solid lines represent the fit of the data to the background model (see text). The most important components of the background (^{210}Bi, ^{90}Sr + ^{90}Y, ^{208}Tl + ^{212}Bi → ^{212}Po, and ^{234m}Pa + ^{214}Bi → ^{214}Po) are shown.

Analysis of the spectrum gives only a limit for the activity of ^{238}U on the level of $\leqslant 0.5$ mBq/kg. The peaks of the daughters ^{234}U, ^{230}Th, and ^{226}Ra cannot be resolved (their Q_α values are very close). A total α peak is expected at energy ≈ 1 MeV. A fit of the spectrum gives only a limit for the total activity of these isotopes at the level of 2.8 mBq/kg. In the same way the following limits on the activities of ^{222}Rn, ^{218}Po, and ^{232}Th were obtained: $\leqslant 4.4$, $\leqslant 4.2$, and $\leqslant 0.7$ mBq/kg, respectively.

To account for the presence in the crystal of β active isotopes (daughters of U/Th, ^{40}K, ^{90}Sr + ^{90}Y), the energy spectrum of the $CaMoO_4$ detector was simulated with the GEANT4 package [45]. The initial kinematics of particles emitted in β decays of nuclei were generated with the DECAY0 event generator [46]. The spectrum of the CMO-2 crystal (Fig. 8) was fitted in the energy interval 0.4–3 MeV by the model, which includes the simulated distributions of U/Th daughters (^{208}Tl, ^{212}Bi → ^{212}Po, ^{210}Bi, ^{214}Bi → ^{214}Po, ^{234m}Pa), ^{40}K, ^{90}Sr + ^{90}Y, Gaussian function to describe the α peak of ^{210}Po, and an exponential function to take into account the external γ background. Parameters of the exponential function were bounded taking into account the background of the $CdWO_4$ crystal scintillator 0.448 kg of mass measured in the set-up [29]. The main components of the background are shown in Fig. 8. Most of the β activity can be ascribed to ^{210}Bi, daughter of ^{210}Pb (≈ 0.4 Bq/kg). We cannot exclude presence of significant activity of ^{90}Sr + ^{90}Y in the crystal. However, there are no clear peculiarities in the spectrum which can be used to prove the presence of these nuclides. Therefore, we can only give limits on activities of ^{90}Sr + ^{90}Y and ^{210}Bi in the crystal at the level of $\leqslant 62$ and $\leqslant 398$ mBq/kg, respectively.

3.6.3. Time–amplitude analysis

The raw background data were analysed using the time-amplitude method, where the energy and arrival time of each event are used to select some decay chains in the ^{232}Th and ^{238}U families.[2] For instance, the following sequence of α decays from the ^{232}Th family was searched for and observed: ^{220}Rn ($Q_\alpha = 6.41$ MeV, $T_{1/2} = 55.6$ s) → ^{216}Po ($Q_\alpha = 6.91$ MeV, $T_{1/2} = 0.145$ s) → ^{212}Pb. These radionuclides are in equilibrium with ^{228}Th from the ^{232}Th family. Because the energy of the α particles from ^{220}Rn decay corresponds to $\simeq 1.5$ MeV in the γ scale of the $CaMoO_4$ detector, the events in the energy region 1.4–2.2 MeV were used as triggers. Then all events (within 1.4–2.2 MeV) following the triggers in the time interval 0.02–0.6 s (containing 84% of ^{216}Po decays) were selected. The obtained α peaks are in agreement with those expected for α particles of ^{220}Rn → ^{216}Po → ^{212}Pb chain [47]. Pulse-shape analysis confirms the events were caused by α particles. On this basis, despite low statistics, the activity of

[2]The technique of a time-amplitude analysis of background data to recognize the presence of the short-lived chains from ^{232}Th, ^{235}U, and ^{238}U families is described in [5,44].

^{228}Th in the $CaMoO_4$ crystal can be calculated as 0.23(10) mBq/kg.

Similarly, for the analysis of the ^{226}Ra chain (^{238}U family) the following sequence of β and α decays was used: ^{214}Bi ($Q_\beta = 3.27$ MeV) → ^{214}Po ($Q_\alpha = 7.83$ MeV, $T_{1/2} = 164\,\mu s$) → ^{210}Pb. For the first event the lower energy threshold was set at 0.25 MeV, while for the events of the α decay of ^{214}Po the energy window 1.4–4 MeV was chosen. The events were selected in the time interval 100−800 μs (55% of ^{214}Po decays). The registration efficiency for events of ^{214}Bi was calculated with the help of the GEANT4 code as 85%. The obtained spectra (Fig. 9) lead to the ^{226}Ra activity in the $CaMoO_4$ crystal equal to 2.1(4) mBq/kg.

The results obtained with time–amplitude analysis do not contradict the results of the analysis described in Section 3.6.2 if one takes into account the broken equilibrium of ^{232}Th and ^{238}U chains.

We estimated the radioactive contamination in other crystals in the same way as described above. A summary of the measured radioactive contamination of the $CaMoO_4$ scintillators (or limits on their activities) is given in Table 4, again in comparison with $CaWO_4$ [29] and $CdWO_4$ detectors [3,6,48,49].

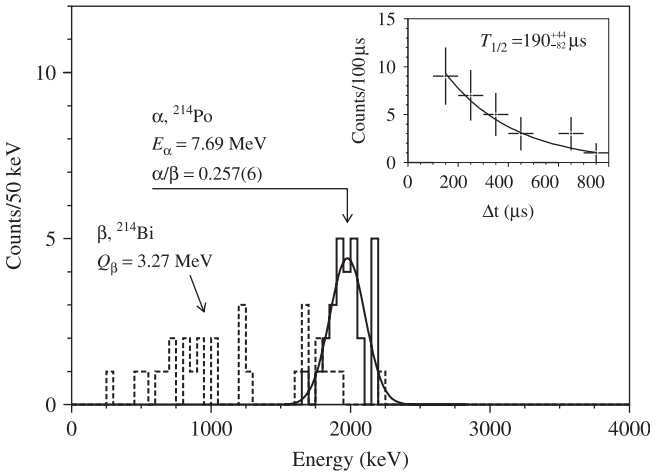

Fig. 9. The energy distributions for the fast sequence of the β (^{214}Bi) and α (^{214}Po) decays selected from the background data by the time-amplitude analysis. (Inset) The time distribution between the first and second events together with an exponential fit. The obtained half-life of ^{214}Po (190^{+44}_{-82} μs) is in agreement with the table value (164 μs) [47].

One can see that the levels of radioactive impurities in the $CaMoO_4$ crystals are comparable with those in $CaWO_4$ crystals, and are much higher (by factor of $10-10^3$) than those in the $CdWO_4$ scintillators. The radioactive contamination of the $CaMoO_4$ crystal produced in the Innovation Centre of Moscow Steel and Alloy Institute is lower than that of the scintillators produced in the Institute for Materials. Some indication that the radioactive contamination in the crystal volume increased during the growth process was observed with the samples CMO-2, CMO-3, and CMO-4 produced from the same crystal boule.

4. High sensitivity ^{100}Mo $0\nu2\beta$ experiment with $CaMoO_4$ detectors

Below we discuss the possible use of $CaMoO_4$ scintillators as detectors in a search for the neutrinoless 2β decay of ^{100}Mo. Because of the "source = detector" approach (which provides high efficiency for detection of the process), good energy resolution and the pulse-shape discrimination ability (which allows us to reduce the background), $CaMoO_4$ scintillators could be considered as a promising tool in a ^{100}Mo $0\nu2\beta$ experiment. To estimate the sensitivity of the experiment, in the following we present calculations of some backgrounds from cosmogenic activities induced in $CaMoO_4$ crystals, as well as from internal pollution by the U/Th chains, and from the two neutrino 2β decays of ^{100}Mo and ^{48}Ca. A natural composition of Ca and O, and 100% enrichment in ^{100}Mo is supposed.

The finite energy resolution of the $CaMoO_4$ detector not only causes a broadening of ^{100}Mo $0\nu2\beta$ peak, but also results in presence of events from tail of the $2\nu2\beta$ distribution in the peak's region. This background is unavoidable because it is caused by ^{100}Mo itself; it could be minimized only by improvement of the energy resolution of the detector. The response functions of $CaMoO_4$ for two neutrino and neutrinoless 2β decays of ^{100}Mo are

Table 4
Radioactive contaminations in $CaMoO_4$, $CaWO_4$, and $CdWO_4$ crystal scintillators

Source	Activity (mBq/kg)					
	CMO-2	CMO-3	CMO-4	CMO-5	CaWO [29]	CdWO [3,6,48,49]
^{232}Th	⩽0.7	⩽0.7	⩽0.9	⩽1.5	0.69(10)	0.053(5)
^{228}Th	0.23(10)	0.42(17)	0.4(4)	0.04(2)	0.6(2)	⩽0.004−0.039(2)
^{238}U	⩽0.5	⩽0.6	⩽0.6	⩽1.5	5.6(5)	⩽0.004
^{226}Ra	2.1(4)	2.5(5)	2.4(1.3)	0.13(4)	5.6(5)	⩽0.004
^{210}Pb	⩽398	⩽401	⩽550	⩽17	⩽430	⩽0.4
^{210}Po	420(10)	490(10)	550(20)	⩽8	291(5)	⩽0.4
^{40}K	⩽1.1	⩽2.1	⩽2.5	⩽3	⩽12	0.3(1)
^{90}Sr	⩽62	⩽178	⩽50	⩽23	⩽70	⩽0.2

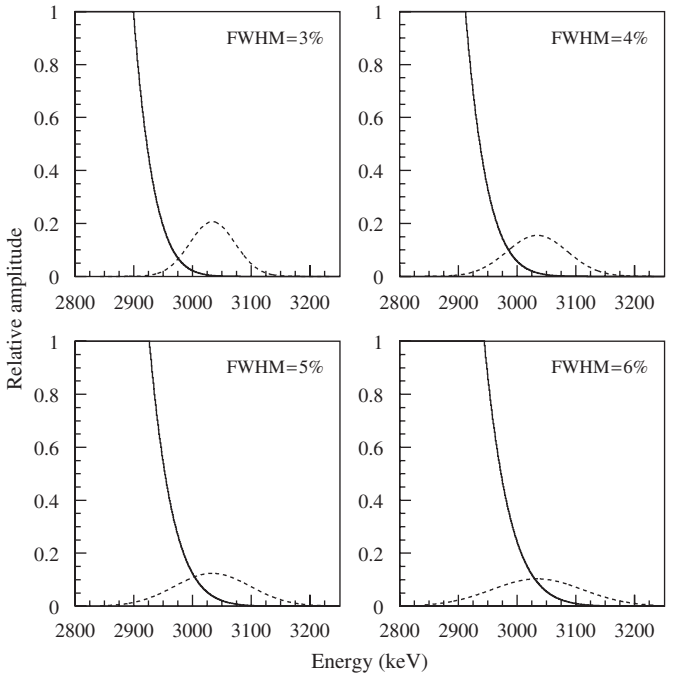

Fig. 10. The response functions of a $Ca^{100}MoO_4$ detector for 2β decays of ^{100}Mo for $T_{1/2}(2\nu) = 7 \times 10^{18}$ yr (solid lines) and $T_{1/2}(0\nu) = 1 \times 10^{24}$ yr (dashed lines) for different energy resolutions of the detector at the energy of ^{100}Mo $0\nu2\beta$ decay.

presented in Fig. 10 for 3%, 4%, 5%, and 6% energy resolution (FWHM) of the detector at the energy of ^{100}Mo $0\nu2\beta$ decay. The amplitude of the $2\nu2\beta$ ($0\nu2\beta$) distribution corresponds to $T_{1/2}(2\nu) = 7 \times 10^{18}$ yr [25] ($T_{1/2}(0\nu) = 1 \times 10^{24}$ yr). It is evident from Fig. 10 that energy resolution should not be worse than 4–5%. For FWHM = 4%, number of events from $2\nu2\beta$ tail in the 1 FWHM energy interval centred at $Q_{2\beta}$ is equal to 0.06 events per kg of $Ca^{100}MoO_4$ per year.

The contribution from the $2\nu2\beta$ decay of ^{48}Ca could be much more dangerous (see Fig. 11). The measured half-life of this process is $T_{1/2}(2\nu) = 4 \times 10^{19}$ yr (see f.e. compilation [20]); ^{48}Ca is present in natural Ca with an abundance of 0.187% [50]. The event rate caused by ^{48}Ca $2\nu2\beta$ decay in the 1 FWHM energy interval is equal to 1.4 events per kg of $Ca^{100}MoO_4$ per year.

In estimating the backgrounds from internal U/Th chains and cosmogenic activities, we additionally suppose the use of an active shield made of CsI(Tl) scintillators. Radiopure CsI(Tl) scintillators were developed by the KIMS collaboration for the dark matter experiments in the Yangyang Laboratory [51]. In simulations, the $CaMoO_4$ crystal ⌀45 × 45 mm was placed in the centre of ⌀40 × 40 cm CsI(Tl) scintillation detector. $CaMoO_4$ was viewed by two PMTs through light-guides also made of CsI(Tl).[3] Such an active shield suppresses internal and external backgrounds related with the emission of γ quanta. The contribution from cosmic ray particles in the course of measurements could be effectively suppressed by running the experiment at a deep underground site.

Only two isotopes in the U/Th chains have enough energy to produce a background in the region of the $0\nu2\beta$ peak of ^{100}Mo: ^{208}Tl ($Q_\beta = 5001$ keV [47]) and ^{214}Bi ($Q_\beta = 3272$ keV).[4] β decay of ^{208}Tl is accompanied by emission of one or more γ quanta, and thus it is effectively eliminated by the CsI(Tl) active shield. β decay of ^{214}Bi is more dangerous because it has a 18.2% branch to the ground state of ^{214}Po without the emission of any γ's and with $Q_\beta = 3272$ keV. However, this contribution could be further suppressed by ≃ 1 order of magnitude by checking for the fast α decay of ^{214}Po ($T_{1/2} = 164.3\,\mu$s) during the subsequent ≃ 1 ms and proving its α nature with pulse-shape analysis. Contributions from ^{208}Tl and ^{214}Bi are shown in Fig. 11 for 0.1 mBq/kg activity. It is clear that they are not very dangerous in comparison with ^{48}Ca $2\nu2\beta$ decay because comparative or better $CaMoO_4$ crystals have already been obtained (CMO-5 in Table 4: 0.04 mBq/kg for ^{208}Tl and 0.13 mBq/kg for ^{214}Bi).

Cosmogenic activities produced by cosmic rays in $Ca^{100}MoO_4$ crystal during its time production period at the Earth surface were calculated with the COSMO code [53]. An activation time of 30 days at sea level, and a deactivation time of 1 year underground were assumed. The most dangerous cosmogenic nuclides—with energy close to or higher than the $Q_{2\beta}$ of ^{100}Mo and noticeable yield—are summarized in Table 5. Simulations with GEANT4 [45] and initial kinematics given by the DECAY0 event generator [46] showed that the contributions from cosmogenic activities are small in comparison with the $2\nu2\beta$ decay of ^{48}Ca (see Fig. 11 for ^{88}Y).

To estimate the sensitivity of the experiment to ^{100}Mo $0\nu2\beta$ decay in terms of the potential half-life limit, we can use known formula: $\lim T_{1/2} = \ln 2 \cdot \eta \cdot N \cdot t / \lim S$, where η is the detection efficiency, N is the number of ^{100}Mo nuclei, t is the measuring time, and $\lim S$ is the maximum number of $0\nu2\beta$ events which can be excluded with a given confidence level on the basis of the experimental data or simulated background. It is interesting to consider here only the unremovable backgrounds from the $2\nu2\beta$ decays of ^{48}Ca and ^{100}Mo itself, neglecting all other external and internal backgrounds (which could be effectively suppressed by the active CsI(Tl) shield).

Supposing measurements with 1 kg $Ca^{100}MoO_4$ scintillator during 1 year, we will have 1.41 (0.06) events from the $2\nu2\beta$ decay of ^{48}Ca (^{100}Mo) inside the 4% 1 FWHM interval centred at the ^{100}Mo $Q_{2\beta}$ energy. In the absence of other contributions, with 1 (or 2) events measured and an expected background of 1.47 events, in accordance with the Feldman–Cousins procedure [54], value of $\lim S$ is equal to 2.9 (4.4) at 90% C.L. Taking into account that this interval contains 0.761 of the full ^{100}Mo $0\nu2\beta$ peak, it gives a

[3] Another possible solution could be light-guides made of $PbWO_4$ scintillators as it was proposed in Ref. [52].

[4] ^{210}Tl is also present with $Q_\beta = 5489$ keV but the yield of this isotope in ^{238}U chain is only 0.021%.

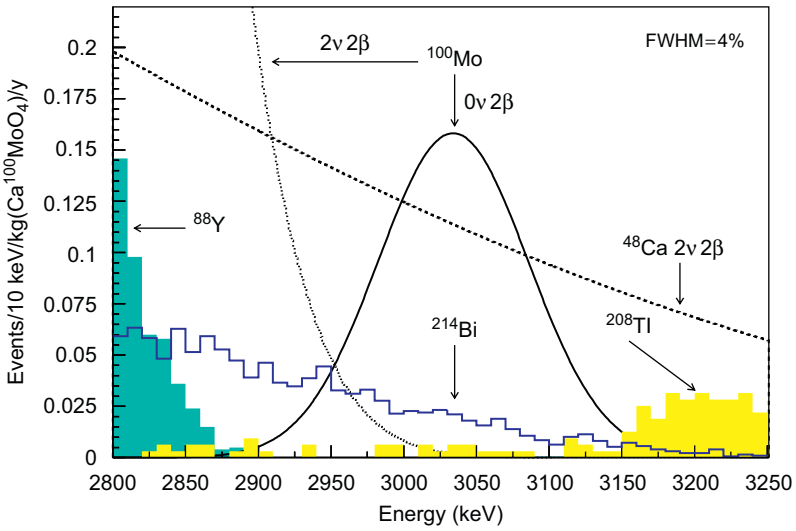

Fig. 11. Calculated backgrounds from the $2\nu2\beta$ decay of ^{48}Ca ($T_{1/2}(2\nu) = 4 \times 10^{19}$ yr), internal pollutions by ^{208}Tl and ^{214}Bi (both with 0.1 mBq/kg), and ^{88}Y isotope from cosmogenic activity. One order of magnitude suppression for ^{214}Bi with the pulse-shape analysis is taken into account. The amplitude of the ^{88}Y distribution in figure corresponds to 1000 decays in $CaMoO_4$, while the expected ^{88}Y cosmogenic activity is only 4 events per kg per year on average during the first 5 years. It is supposed that the $Ca^{100}MoO_4$ scintillator is operating in anticoincidence with the CsI(Tl) active shield (see text). Distributions for ^{100}Mo are shown for $T_{1/2}(2\nu) = 7 \times 10^{18}$ yr and $T_{1/2}(0\nu) = 1 \times 10^{24}$ yr.

Table 5
Cosmogenic radioactivity induced in $Ca^{100}MoO_4$ crystals, assuming a 30 days exposure to cosmic rays at the sea level and 1 yr period of cooling down in underground conditions

Isotope or chain of decays	$T_{1/2}$	Decay mode and Q value (keV)		D_5
^{22}Na	2.6 yr	EC	2842	8.99
^{42}Ar and ^{42}K	32.9 yr	β^-	3525	0.80
^{56}Co	77.3 d	EC	4565	0.01
^{60}Co	5.3 yr	β^-	2824	2.08
^{68}Ge and ^{68}Ga	270.8 d	EC	2921	0.90
^{88}Y	106.7 d	EC	3623	20.69

D_5 is number of decays during the first 5 years of data taking per kg of the crystal.

half-life limit as: $T_{1/2}(0\nu) > 5.4 \times 10^{23} (3.5 \times 10^{23})$ yr. Thus, comparatively modest efforts with a 1 kg crystal (which contains near 490 g of ^{100}Mo) and a 1 yr measurement time could give an interesting $T_{1/2}$ limit comparable to the recent value from the NEMO-3 experiment: 4.6×10^{23} yr [25] obtained with 7 kg of ^{100}Mo after 389 d of data taking.

The final aim of the NEMO-3 experiment ($T_{1/2}(0\nu) > 2 \times 10^{24}$ yr) could be achieved with a $Ca^{100}MoO_4$ scintillator with statistics of 10 kg yr, i.e. also in a middle-scale experiment. However, further improvement will be difficult task: the half-life limit of 10^{25} yr could be reached only with 200 kg yr statistics. More sensitive searches for ^{100}Mo $0\nu2\beta$ decay will evidently need the depletion of Ca in ^{48}Ca.[5]

[5]Only 20 years ago, before the first laboratory observation of $2\nu2\beta$ decay in 1987, it was difficult to imagine that this rarest observed natural process could be a serious background in searches for even rarer decays.

$CaMoO_4$ crystals could also be used as scintillating bolometers [17]. In this case energy resolution will be much better ($\simeq$ 5 keV instead of $\simeq$ 120 keV for 4%) that results in a clearer interpretation of the backgrounds and a higher sensitivity of an experiment. Two neutrino 2β decay of ^{100}Mo will not contribute anymore to the $0\nu2\beta$ peak. With background only from $2\nu2\beta$ decay from non-depleted ^{48}Ca, the following half-life limits could be reached (at 90% C.L.): 6.5×10^{23}, 4.1×10^{24}, and 4.2×10^{25} yr for 1, 10 and 200 kg yr statistics, respectively. Statistics of 1000 kg yr would correspond to $T_{1/2}(0\nu) > 1.1 \times 10^{26}$ yr. In accordance with the NME calculations for ^{100}Mo $0\nu2\beta$ decay [20,21], it will give a sensitivity on the effective neutrino mass in the range of 0.03–0.20 eV.

A R&D programme with the aim to developing low-background, high resolution scintillation detector for an experiment to search for the $0\nu2\beta$ decay of ^{100}Mo with a sensitivity at the level of 10^{25} yr is in progress. For this purpose we intend to produce larger $CaMoO_4$ crystals up to 45 mm in diameter and up to 80–100 mm in length.

5. Conclusions

The scintillation properties and the radioactive contamination of $CaMoO_4$ crystals produced by the Institute for Materials (Lviv, Ukraine), and by the Innovation Centre of Moscow Steel and Alloy Institute (Moscow, Russia) have been studied.

The energy resolutions 10.3% and 4.7% for the 662 and 2615 keV γ lines were obtained with the $CaMoO_4$ sample of $\oslash 38 \times 20$ mm produced by the Institute for Materials. The photoelectron yield of $CaMoO_4$ at room temperature was measured as 36% of $CaWO_4$, and $\approx$ 8% of NaI(Tl).

The α/β ratio was measured with α particles from a ^{241}Am α source, and internal U/Th contamination.

Three components of the scintillation decay ($\tau_i \approx 0.3-1$, ≈ 4 and $\approx 17\,\mu$s at the temperature 27 °C) and their intensities under α particles and γ quanta irradiation were measured. Some difference in pulse shapes allows to discriminate α particles and γ quanta with reasonable efficiency.

The temperature dependence of the light output and pulse shape was measured in temperature range $-175 \div +40\,^{\circ}$C. At approximately $-50\,^{\circ}$C the light output increases ≈ 2 times compared to the light output at room temperature.

The radioactive contamination of $CaMoO_4$ crystals was estimated in low background measurements carried out in the Solotvina Underground Laboratory. $CaMoO_4$ scintillators produced in the Institute for Materials (Lviv, Ukraine) show a significant contamination by uranium and thorium (particularly by ^{210}Po at the level of $\approx 0.4-0.5$ Bq/kg). The contamination of the $CaMoO_4$ crystal produced by the Innovation Centre of the Moscow Steel and Alloy Institute (Moscow, Russia) is 1–2 orders of magnitude better. It was found that the equilibrium in the uranium chains is broken in $CaMoO_4$ crystals. Some indication that the level of radioactive contamination in the crystal volume increased during the growth process was observed.

Perspectives for a high sensitivity experiment to search for the $0\nu2\beta$ decay of ^{100}Mo are discussed. The energy resolution of 4–5% is enough to reach a sensitivity at the level of 10^{25} yr. The contamination of crystals by ^{226}Ra and ^{232}Th should not exceed the level of 0.1 mBq/kg. The two neutrino 2β decay of ^{48}Ca restricts the sensitivity of an experiment to search for the $0\nu2\beta$ decay of ^{100}Mo using $CaMoO_4$ crystal scintillators. A possible solution would be to produce $CaMoO_4$ scintillators from Calcium depleted in ^{48}Ca. A further improvement of sensitivity could be achieved by using $CaMoO_4$ crystals as scintillating bolometers.

Acknowledgements

Work of A.N. Annenkov, O.A. Buzanov, V.N. Kornoukhov, M. Korzhik, and O. Missevitch was supported in part by ISTC project #3293 in collaboration with the Dark Matter Research Center and School of Physics of Seoul National University, Republic of Korea. F.A. Danevich, V.V. Kobychev, V.M. Mokina, S.S. Nagorny, A.S. Nikolaiko, D.V. Poda, R.B. Podviyanuk, D.J. Sedlak, O.G. Shkulkova, V.I. Tretyak, S.S. Yurchenko were supported in part by the Project "Kosmomikrofizyka" (Astroparticle physics) of the National Academy of Sciences of Ukraine. We acknowledge S. Henry for his remarks regarding this manuscript.

References

[1] F.A. Danevich, et al., Instrum. Exp. R. 32 (1989) 1059.
[2] S.F. Burachas, et al., Phys. At. Nucl. 58 (1995) 153.
[3] F.A. Danevich, et al., Z. Phys. A 355 (1996) 433.
[4] P. Belli, et al., Nucl. Phys. B 563 (1999) 97.
[5] F.A. Danevich, et al., Nucl. Phys. A 694 (2001) 375.
[6] F.A. Danevich, et al., Phys. Rev. C 68 (2003) 035501.
[7] P. Belli, et al., Nucl. Instr. and Meth. A 498 (2003) 352.
[8] I. Ogawa, et al., Nucl. Phys. A 730 (2004) 215.
[9] F.A. Danevich, et al., Nucl. Instr. and Meth. A 544 (2005) 553.
[10] R. Bernabei, et al., Phys. Lett. B 546 (2002) 23.
[11] S. Belogurov, et al., IEEE Nucl. Sci. NS-52 (2005) 1131;
H.J. Kim et al., in: Proceedings of New View in Particle Physics (VIETNAM'2004), August 5–11, 2004, p. 449.
[12] V.B. Mikhailik, et al., Phys. Status Solidi B 242 (2005) R17.
[13] V.B. Mikhailik, et al., J. Appl. Phys. 97 (2005) 083523.
[14] V.B. Mikhailik, et al., J. Phys. Condens. Matter 17 (2005) 7209.
[15] A. Senyshyn, et al., Phys. Rev. B 73 (2006) 014104.
[16] V.B. Mikhailik, H. Kraus, J. Phys. D Appl. Phys. 39 (2006) 1181.
[17] S. Pirro, et al., Phys. At. Nucl. 69 (2006) 2109.
[18] M. Doi, et al., Prog. Theor. Phys. Suppl. 83 (1985) 1.
[19] J. Suhonen, O. Civitarese, Phys. Rep. 300 (1998) 123.
[20] V.I. Tretyak, Yu.G. Zdesenko, At. Data Nucl. Data Tables 61 (1995) 43;
V.I. Tretyak, Yu.G. Zdesenko, At. Data Nucl. Data Tables 80 (2002) 83.
[21] F. Simkovic, et al., Phys. Rev. C 64 (2001) 035501;
S. Stoica, V.P. Paun, Rom. J. Phys. 47 (2002) 497;
J. Suhonen, Nucl. Phys. A 700 (2002) 649;
O. Civitarese, J. Suhonen, Nucl. Phys. A 729 (2003) 867;
V.A. Rodin, et al., Phys. Rev. C 68 (2003) 044302;
V.A. Rodin, et al., Nucl. Phys. A 766 (2006) 107;
V.A. Rodin, et al., Erratum, Nucl. Phys. A 793 (2007) 213.
[22] G. Pantis, et al., Phys. Rev. C 53 (1996) 695.
[23] Yu.G. Zdesenko, et al., Astropart. Phys. 23 (2005) 249.
[24] S.I. Vasil'ev, et al., JETP Lett. 51 (1990) 622;
H. Ejiri, et al., Phys. Lett. B 258 (1991) 17;
D. Dassie, et al., Phys. Rev. D 51 (1995) 2090;
M. Alston-Garnjost, et al., Phys. Rev. C 55 (1997) 474;
A. De Silva, et al., Phys. Rev. C 56 (1997) 2451;
V.D. Ashitkov, et al., JETP Lett. 74 (2001) 529.
[25] R. Arnold, et al., Phys. Rev. Lett. 95 (2005) 182302.
[26] H. Hidaka, C.V. Ly, K. Suzuki, Phys. Rev. C 70 (2004) 025501.
[27] A.S. Barabash, et al., Phys. Lett. B 345 (1995) 408;
A.S. Barabash, et al., Phys. At. Nucl. 62 (1999) 2039;
M.J. Hornish, et al., Phys. Rev. C 74 (2006) 044314;
R. Arnold, (NEMO Collaboration), et al., Nucl. Phys. A 781 (2006) 209.
[28] P. Belli et al., in: Proceedings of the International Conference on Current Problems in Nuclear Physics and Atomic Energy (NPAE'2006), May 29–June 3, 2006, Ukraine—Kyiv INR, Kyiv, 2007, p. 479.
[29] Yu.G. Zdesenko, et al., Nucl. Instr. and Meth. A 538 (2005) 657.
[30] L. Bardelli, et al., Nucl. Instr. and Meth. A 569 (2006) 743.
[31] C. Palache, H. Berman, C. Frondel, The System of Mineralogy, seventh ed., vol. II, Wiley, New York, 1951.
[32] A. Petrov, P. Kofstad, J. Solid State Chem. 30 (1979) 83;
M.V. Mokhosoev, J.G. Bazarova, Complex Oxides of Molybdenum and Tungsten with Elements of the I–IV Groups, Nauka, Moscow, 1990;
I.S. Grigoriev, et al. (Eds.), Physical Quantities, Energoatomizdat, Moscow, 1991.
[33] E.N. Farabaugh, H.S. Peiser, J.B. Wachtman Jr., J. Res. Nat. Bur. Stand. A 70 (1966) 379.
[34] T. Fazzini, et al., Nucl. Instr. and Meth. A 410 (1998) 213.
[35] F.A. Danevich, et al., Phys. Rev. C 67 (2003) 014310.
[36] J.B. Birks, Theory and Practice of Scintillation Counting, Pergamon Press, London, 1964.
[37] E. Gatti, F. De Martini, in: Nuclear Electronics 2, IAEA, Vienna, 1962, p. 265.
[38] F.A. Danevich, et al., Nucl. Instr. and Meth. A 541 (2005) 583.

[39] P. Belli, et al., Nucl. Phys. A 789 (2007) 15.
[40] L. Bardelli et al., arXiv:0706.2422[nucl-ex];
L. Bardelli, et al., Nucl. Instr. and Meth. A, 2007, in press, doi:10.1016/j.nima.2007.10.021.
[41] V.B. Mikhailik et al., Nucl. Instr. and Meth. A, 2007, in press, doi:10.1016/j.nima.2007.09.020.
[42] S.B. Mikhrin, et al., Nucl. Instr. and Meth. A 486 (2002) 295.
[43] Yu.G. Zdesenko, et al., in: Proceedings of the 2nd International Symposium on Underground Physics, Baksan Valley, USSR, August 17–19, 1987, Moscow, Nauka, 1988, p. 291.
[44] F.A. Danevich, et al., Phys. Lett. B 344 (1995) 72.
[45] S. Agostinelli, et al., Nucl. Instr. and Meth. A 506 (2003) 250;
J. Allison, et al., IEEE Trans. Nucl. Sci. NS-53 (2006) 270.
[46] O.A. Ponkratenko, V.I. Tretyak, Yu.G. Zdesenko, Phys. At. Nucl. 63 (2000) 1282;
V.I. Tretyak, to be published.
[47] R.B. Firestone, et al., Table of Isotopes, eighth ed., Wiley, New York, 1996 and CD update, 1998.
[48] A.Sh. Georgadze, et al., Instrum. Exp. Tech. 39 (1996) 191.
[49] S.Ph. Burachas, et al., Nucl. Instr. and Meth. A 369 (1996) 164.
[50] J.K. Bohlke, et al., J. Phys. Chem. Ref. Data 34 (2005) 57.
[51] H.S. Lee, et al., Phys. Lett. B 633 (2006) 201;
H.S. Lee, et al., Nucl. Instr. and Meth. A 571 (2007) 644.
[52] F.A. Danevich, et al., Nucl. Instr. and Meth. A 556 (2006) 259.
[53] C.J. Martoff, P.D. Lewin, Comput. Phys. Commun. 72 (1992) 96.
[54] G.J. Feldman, R.D. Cousins, Phys. Rev. D 57 (1998) 3873.